HAL
open science

Isofulminic acid, HONC: Ab initio theory and microwave spectroscopy

M. Mladenovic, Marius Lewerenz, M.C. Mccarthy, P. Thaddeus

To cite this version:

M. Mladenovic, Marius Lewerenz, M.C. Mccarthy, P. Thaddeus. Isofulminic acid, HONC: Ab initio theory and microwave spectroscopy. The Journal of Chemical Physics, 2009, 131 (17), pp.174308. 10.1063/1.3257680 . hal-00750631

HAL Id: hal-00750631

https://hal.science/hal-00750631

Submitted on 12 Nov 2012

HAL is a multi-disciplinary open access archive for the deposit and dissemination of scientific research documents, whether they are published or not. The documents may come from teaching and research institutions in France or abroad, or from public or private research centers.

L'archive ouverte pluridisciplinaire **HAL**, est destinée au dépôt et à la diffusion de documents scientifiques de niveau recherche, publiés ou non, émanant des établissements d'enseignement et de recherche français ou étrangers, des laboratoires publics ou privés.

The Journal of Chemical Physics

Isofulminic acid, HONC: Ab initio theory and microwave spectroscopy

Mirjana Mladenović, Marius Lewerenz, Michael C. McCarthy, and Patrick Thaddeus

Citation: J. Chem. Phys. **131**, 174308 (2009); doi: 10.1063/1.3257680
View online: http://dx.doi.org/10.1063/1.3257680
View Table of Contents: http://jcp.aip.org/resource/1/JCPSA6/v131/i17
Published by the American Institute of Physics.

Additional information on J. Chem. Phys.

Journal Homepage: http://jcp.aip.org/
Journal Information: http://jcp.aip.org/about/about_the_journal
Top downloads: http://jcp.aip.org/features/most_downloaded
Information for Authors: http://jcp.aip.org/authors

ADVERTISEMENT

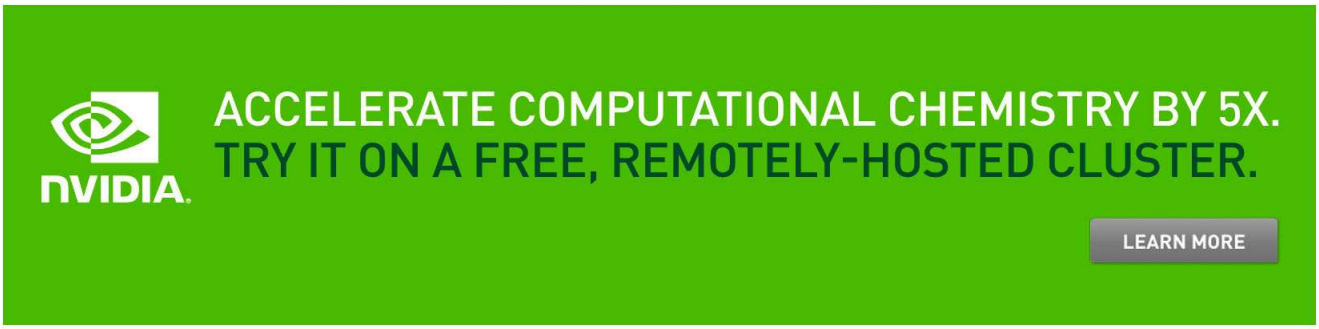

Downloaded 11 Nov 2012 to 129.132.209.87. Redistribution subject to AIP license or copyright; see http://jcp.aip.org/about/rights_and_permissions

Isofulminic acid, HONC: *Ab initio* theory and microwave spectroscopy

Mirjana Mladenović,[1,a)] Marius Lewerenz,[1,b)] Michael C. McCarthy,[2,c)] and Patrick Thaddeus[2,d)]

[1]*Laboratoire Modélisation et Simulation Multi Echelle, MSME FRE3160 CNRS, Université Paris-Est, 5 bd Descartes, 77454 Marne la Vallée, Cedex 2, France*

[2]*Harvard-Smithsonian Center for Astrophysics, 60 Garden Street, Cambridge, Massachusetts 02138, USA and School of Engineering and Applied Sciences, Harvard University, Cambridge, Massachusetts 02138, USA*

(Received 25 June 2009; accepted 9 October 2009; published online 4 November 2009)

Isofulminic acid, HONC, the most energetic stable isomer of isocyanic acid HNCO, higher in energy by 84 kcal/mol, has been detected spectroscopically by rotational spectroscopy supported by coupled cluster electronic structure calculations. The fundamental rotational transitions of the normal, carbon-13, oxygen-18, and deuterium isotopic species have been detected in the centimeter band in a molecular beam by Fourier transform microwave spectroscopy, and rotational constants and nitrogen and deuterium quadrupole coupling constants have been derived. The measured constants agree well with those predicted by *ab initio* calculations. A number of other electronic and spectroscopic parameters of isofulminic acid, including the dipole moment, vibrational frequencies, infrared intensities, and centrifugal distortion constants have been calculated at a high level of theory. Isofulminic acid is a good candidate for astronomical detection with radio telescopes because it is highly polar and its more stable isomers (HNCO, HOCN, and HCNO) have all been identified in space. © *2009 American Institute of Physics*. [doi:10.1063/1.3257680]

I. INTRODUCTION

Isocyanic acid and its isomers have long attracted organic chemists because they are composed of the four most important biogenic elements of organic chemistry, and because they provide interesting tests of chemical bonding and electronic structure. The isocyanic acid isomers have been the subject of theoretical and experimental studies since the 16th century.[1] Although many isomeric arrangements are possible, only four are minima on the potential energy surface:[2–4] isocyanic acid HNCO, cyanic acid HOCN, fulminic acid HCNO, and isofulminic acid HONC. All have singlet electronic ground states, linear or nearly linear heavy-atom backbones, and planar equilibrium structures.[3–5] Recent calculations[5] predict that HOCN, HCNO, and HONC lie, respectively, 24.7, 70.7, and 84.1 kcal/mol higher in energy than HNCO. All are calculated to be highly polar molecules, with dipole moments from 1 to 3.5 D.[6,7]

The isocyanic isomers are of astronomical interest. Isocyanic acid itself was one of the first molecules[8] identified in the interstellar gas on the basis of the prior laboratory microwave spectroscopy.[9] It has now been found in many locations, including over sixty galactic sources and nine external galaxies.[10–14] On the basis of recent laboratory data, there is now evidence for cyanic acid in the Galactic center source Sgr B2;[15,16] at about the same time, Marcelino *et al.*[17] observed radio lines of the third most stable isomer, fulminic acid, in three starless cores and in the low-mass star forming region L1527. The presence of higher-lying isomers in hot cores and other warm regions may result from reactions on the surfaces of interstellar dust grains. If so, the isocyanic isomers may provide a useful tool to estimate relative contributions of gas-phase and grain chemistry.

Until quite recently, only isocyanic acid and fulminic acid had been detected at high spectral resolution in the gas phase. The rotational and vibrational spectra of both have now been thoroughly studied,[18,19] motivated partly by a desire to understand the quasilinear structure produced by the large-amplitude bending motion. The second most stable isomer, cyanic acid HOCN, was first detected at low temperature in an inert matrix after ultraviolet irradiation of HNCO,[20] work extended by Bondybey *et al.*,[21] who showed that irradiation of HCNO in a matrix also yields HOCN. During the past year, cyanic acid has been detected in the gas phase, and its microwave rotational spectrum measured.[15]

Until the present work, there was no conclusive evidence for the remaining isomer, isofulminic acid HONC. Maier *et al.*[22] reported a low temperature infrared matrix spectrum in argon, but the assignment was subsequently withdrawn.[23] There have been at least two attempts to produce HONC by pyrolysis of mercury fulminate and other compounds; the first by Wentrup *et al.*[24] only produced HCNO and trace amounts of HNCO; the second by McNaughton and Evans[25] yielded a weak feature near the predicted frequency of the $3_{0,3} \rightarrow 2_{0,2}$ rotational transition of HONC, without confirming lines. No lines attributable to HOCN were observed.

From theoretical self-consistent field (SCF) calculations of the potential energy surface of the isocyanic isomers, Poppinger *et al.*[3] and McLean *et al.*[2] concluded that isofulminic

[a)]Author to whom correspondence should be addressed. Electronic mail: mladenov@univ-mlv.fr.
[b)]Electronic mail: lewerenz@univ-mlv.fr.
[c)]Electronic mail: mccarthy@cfa.harvard.edu.
[d)]Electronic mail: pthaddeus@cfa.harvard.edu.

 © 2009 American Institute of Physics

Downloaded 11 Nov 2012 to 129.132.209.87. Redistribution subject to AIP license or copyright; see http://jcp.aip.org/about/rights_and_permissions

acid is stable enough to exist in the interstellar gas. Poppinger *et al.*[26] also examined substituted isocyanic acid isomers, in particular the stability of the lesser known RONC isomers, first experimentally observed by Wentrup *et al.*[27] three years later. Pinnavaia *et al.*[4] used a perturbational approach to calculate spectroscopic parameters of HONC from a quartic internal coordinate force field determined by second order Møller–Plesset theory. Isomerization and fragmentation pathways for the CHNO system were studied by Mebel *et al.*[28] with density functional theory, by Ding *et al.*[29] with the complete active space method, and by Schuurman *et al.*[5] with several coupled cluster approaches. The equilibrium geometry and energetics of the four most stable isocyanic isomers were recently analyzed in significant detail by some of the present authors with the all electron coupled cluster singles and doubles with perturbative triple excitations, CCSD(T) method, in combination with large correlation consistent bases.[6,30] The computed barriers to linearity from all electron CCSD(T)/aug-cc-pCVQZ calculations are 5.3 kcal/mol (1839 cm^{-1}) for HNCO, 26.9 kcal/mol (9406 cm^{-1}) for HOCN, and 47.9 kcal/mol (16761 cm^{-1}) for HONC, whereas the equilibrium structure of HCNO was calculated to be linear. In addition, HOCN, HCNO, and HONC were found to lie 24.5 kcal/mol (8577 cm^{-1}), 70.0 kcal/mol (24467 cm^{-1}), and 84.2 kcal/mol (29464 cm^{-1}) above the most stable HNCO molecule, in good agreement (to 0.2 kcal/mol) with the earlier frozen-core focal-point analysis results of Schuurman *et al.*[5] Minimum energy paths along the angular coordinates were used in combination with the dominant kinetic energy contributions to predict their key rovibrational spectroscopic features.[30] The harmonic heavy-atom bending frequency ω_5 and the harmonic torsional frequency ω_6 of HONC were identified as the lowest among all of the four stable CHNO isomers.[6,30] Their electric and magnetic properties were studied in Ref. 7, where both a Mulliken population analysis of the total electron density and molecular orbitals were used to interpret the changes in the electronic structure properties.

Motivated by the recent gas-phase detection of cyanic acid[15] and coupled cluster calculations,[6,7,30] a combined experimental and theoretical effort has been undertaken to spectroscopically characterize the most energetic isomer, isofulminic acid. Here we report the laboratory detection of the fundamental rotational transition of HONC in a supersonic molecular beam by Fourier transform microwave (FTM) spectroscopy. Our identification has been confirmed by detection of the same transition in the carbon-13, oxygen-18, and deuterium isotopic species, with the expected nitrogen hyperfine structure. A number of other spectroscopic quantities including equilibrium and ground state rotational constants, dipole moments, anharmonic vibrational frequencies, infrared intensities, and centrifugal distortion constants have also been calculated theoretically for HONC and its rare isotopologues.

II. THEORETICAL CALCULATIONS

Ab initio calculations have been carried out for the ground A' electronic state by means of the coupled cluster electron correlation method CCSD(T) including all single and double excitations and a perturbative term for connected triple substitutions, as implemented in the Mainz–Austin–Budapest version of the ACES2 program package.[31] Dunning's correlation consistent polarized core valence basis sets, commonly termed cc-pCVXZ, have been used.[32,33]

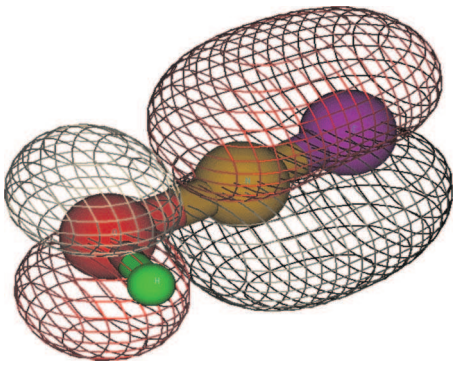

FIG. 1. Highest occupied molecular $2a''$ orbital of HONC. The contour surfaces of orbital amplitude 0.025 and −0.025 are shown.

HONC possesses a planar equilibrium structure of *trans* type.[7] In C_s symmetry, the reference electronic configuration used in the SCF approximation to construct molecular orbitals is given by

$$(\text{core})^6(4a')^2(5a')^2(6a')^2(7a')^2(1a'')^2(8a')^2(9a')^2(2a'')^2,$$

where the core contribution $(1a')^2(2a')^2(3a')^2$ contains the three $1s$-like core orbitals located on oxygen, nitrogen, and carbon, respectively. The highest occupied molecular $2a''$ orbital is primarily composed of the out-of-plane $2p_x$ atomic orbitals of O, C, and N, as depicted in Fig. 1, where a lone electron pair on oxygen may easily be noted. The dominant single determinant reference character is confirmed by a T_1 diagnostic value near 0.014 and largest $|T_2|$ amplitudes smaller than 0.07 in our all electron CCSD(T) calculations.

A. Equilibrium geometry

Large-scale coupled cluster CCSD(T) all electron results for the equilibrium structure of HONC were reported in a recent study on the CHNO isomer family.[30] There the geometrical parameters at the complete basis set (CBS) limit, computed for the cc-pCVXZ and aug-cc-pCVXZ basis set families by means of the simple three-parameter exponential extrapolation, showed excellent agreement within 0.0003 a_0, 0.02° [∠(ONC)], and 0.07° [∠(HON)]. The best estimate for the heavy atom ONC bond angle of 172.56°, introduced in Ref. 30 as the mean value of the two respective CBS results, is employed in the present work in combination with the CCSD(T)/cc-pCV∞Z bond lengths and the mean value of 104.92° for the HON angle, where ∞ denotes the CBS limit. The latter set of geometrical parameters is displayed in Fig. 2 and will be referred to as the best estimate geometry. For quantities computed at this geometrical arrangement, we use the superscript ∞ throughout this paper.

The NC bond length in Fig. 2 is only 0.004 Å longer than r(NC) of 1.169 Å in HNC,[34] indicating a similar type of bonding ($N^+ \equiv C^-$) in the two molecules. This is in accord with a partial atomic charge (δ) distribution found to be

Downloaded 11 Nov 2012 to 129.132.209.87. Redistribution subject to AIP license or copyright; see http://jcp.aip.org/about/rights_and_permissions

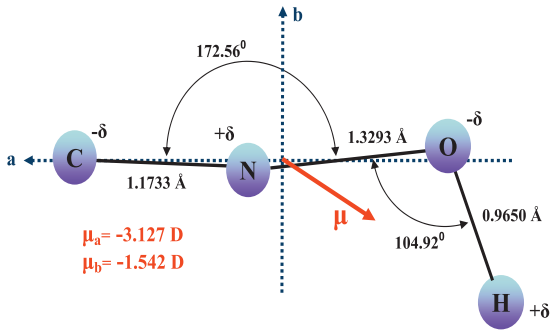

FIG. 2. *Ab initio* equilibrium structure, principal a,b moment-of-inertia axes and dipole moment vector μ.

+0.31, −0.24, +0.14, and −0.21 e along the H-O-N-C chain from the atomic population analysis of the CCSD(T)/cc-pCV5Z density (see Sec. II D). One may also note that the H-O-N angle in Fig. 2 compares well with the H-O-H angle of 104.45° in H_2O,[35] what presumably points at a similar spatial electron distribution around oxygen in HONC and H_2O.

The a principal inertial axis in Fig. 2 lies rather close to the nearly linear heavy-atom ONC backbone of the molecule, rotated only 4.8° from the N–O bond. The CCSD(T)/cc-pCV5Z dipole moment vector for the best estimate structure has a magnitude of $|\mu|=3.487$ D. This value is somewhat smaller than $|\mu|=3.815$ D for HOCN and larger than $|\mu|=3.340$ for HCNO and $|\mu|=2.073$ D for HNCO, calculated at the same CCSD(T)/cc-pCV5Z level of theory.[7] In addition, $|\mu|$ of HONC is somewhat larger than the CCSD(T)/aug-cc-pCVQZ dipole moment of 3.110 D calculated here for HNC. The experimentally derived $|\mu|$ values for HNCO, HCNO, and HNC are 2.075 D (Ref. 36), 3.350 D (Ref. 37), and 3.050 D (Ref. 38), respectively.

B. Spectroscopic parameters

Zero point vibrational corrections to rotational constants could be computed only at the CCSD(T)/cc-pCVTZ level due to technical limitations. The equilibrium rotational constants calculated from the CCSD(T)/cc-pCVTZ optimum geometry reported previously[30] and from the best estimate structure of Fig. 2 are collected for the five HONC isotopologues in Table I. The former set of constants is denoted by $A_e^{(3)},B_e^{(3)},C_e^{(3)}$, whereas we use $A_e^{(\infty)},B_e^{(\infty)},C_e^{(\infty)}$ to designate the latter results. As seen, HONC is an almost prolate symmetric top with an asymmetry parameter κ of −0.9994. The ground-state rotational constants $A_0^{(3)},B_0^{(3)},C_0^{(3)}$ and ground-state vibrational corrections $\Delta A^{(3)},\Delta B^{(3)},\Delta C^{(3)}$ are both obtained from the CCSD(T)/cc-pCVTZ calculations carried out at the CCSD(T)/cc-pCVTZ optimum geometry. The ground-state vibrational corrections are computed from the cubic and semidiagonal quartic force field in a normal coordinate representation by means of vibrational second-order perturbation theory.[39]

The ground-state rotational constants for the best CCSD(T) estimate structure are obtained from $A_e^{(\infty)},B_e^{(\infty)},C_e^{(\infty)}$ and the ground-state CCSD(T)/cc-pCVTZ vibrational corrections according to

TABLE I. Experimental and theoretical rotational constants. Equilibrium rotational constants A_e,B_e,C_e, ground-state rotational constants A_0,B_0,C_0, and ground-state vibrational corrections $\Delta A,\Delta B,\Delta C$ are calculated from the CCSD(T)/cc-pCVTZ optimum structure (superscript 3) and the best CCSD(T) estimate structure (superscript ∞). The experimentally derived rotational constants $B_{\rm eff}$ for the $K_a=0$ ladder are highlighted by bold numbers. The numbers in parentheses given along with the experimental values are the estimated uncertainties (1σ) in units of the last significant digit. For the definition of $\bar{B}_{\rm eff}^{(\infty,3)}$ and $\Delta(B_{\rm eff})$, see Eqs. (2) and (3). All quantities are given in megahertz.

Property	HONC	DONC	HON^{13}C	HO^{15}NC	H^{18}ONC
$A_e^{(3)}$	616 751	341 630	616 606	615 722	609 174
$\Delta A^{(3)}$	−1888	1222	−1981	−2326	−2486
$A_0^{(3)}$	618 638	340 407	618 586	618 048	611 660
$B_e^{(3)}$	11 025	10 547	10 592	11 015	10 471
$\Delta B^{(3)}$	36	27	34	36	34
$B_0^{(3)}$	10 989	10 519	10 558	10 979	10 437
$C_e^{(3)}$	10 831	10 231	10 413	10 821	10 294
$\Delta C^{(3)}$	51	46	47	51	47
$C_0^{(3)}$	10 781	10 185	10 366	10 770	10 247
$A_e^{(\infty)}$	622 335	345 246	622 186	621 255	614 597
$B_e^{(\infty)}$	11 107	10 619	10 671	11 097	10 549
$C_e^{(\infty)}$	10 912	10 302	10 491	10 902	10 371
$A_0^{(\infty,3)}$	624 223	344 024	624 167	623 581	617 083
$B_0^{(\infty,3)}$	11 071	10 592	10 637	11 061	10 515
$C_0^{(\infty,3)}$	10 861	10 256	10 444	10 851	10 330
$\bar{B}_{\rm eff}^{(\infty,3)}$	10 966	10 424	10 540	10 956	10 422
$B_{\rm eff}$	**10 953.3904(4)**	**10 411.8238(6)**	**10 528.2985(6)**		**10 407.98704(6)**
$\Delta(B_{\rm eff})$	13	12	12		14

Downloaded 11 Nov 2012 to 129.132.209.87. Redistribution subject to AIP license or copyright; see http://jcp.aip.org/about/rights_and_permissions

TABLE II. CCSD(T)/cc-pCVTZ harmonic ω_i and fundamental ν_i vibrational frequencies (in cm^{-1}), as well as the infrared intensity I (in km/mol), computed for the CCSD(T)/cc-pCVTZ optimum geometry.

Property	HONC	DONC	$HON^{13}C$	$HO^{15}NC$	$H^{18}ONC$
$\omega_1(a')$	3770	2746	3770	3770	3758
$\omega_2(a')$	2170	2167	2137	2129	2168
$\omega_3(a')$	1435	1070	1434	1433	1430
$\omega_4(a')$	968	966	957	964	936
$\omega_5(a')$	252	245	250	246	251
$\omega_6(a'')$	305	300	302	298	303
$\nu_1(a')$	3584	2648	3584	3584	3573
$\nu_2(a')$	2128	2125	2095	2089	2126
$\nu_3(a')$	1393	1047	1392	1392	1389
$\nu_4(a')$	949	947	938	945	917
$\nu_5(a')$	273	257	270	267	271
$\nu_6(a'')$	321	308	318	314	319
$I(\nu_1)$	108	54	108	108	108
$I(\nu_2)$	20	17	18	20	21
$I(\nu_3)$	60	38	61	60	58
$I(\nu_4)$	41	35	40	41	39
$I(\nu_5)$	4	4	4	4	4
$I(\nu_6)$	6	1	6	6	6

$$A_0^{(\infty,3)} = A_e^{(\infty)} - \Delta A^{(3)}, \tag{1}$$

and by analogy for B and C. For comparison with the experimental results B_{eff} reported in Table I, we introduce the average value $\bar{B}_{\text{eff}}^{(\infty,3)}$,

$$\bar{B}_{\text{eff}}^{(\infty,3)} = [B_0^{(\infty,3)} + C_0^{(\infty,3)}]/2, \tag{2}$$

and the deviation ΔB_{eff},

$$\Delta(B_{\text{eff}}) = \bar{B}_{\text{eff}}^{(\infty,3)} - B_{\text{eff}} \tag{3}$$

of the theoretical results $\bar{B}_{\text{eff}}^{(\infty,3)}$ from the experimental counterparts B_{eff}. Table I shows that the *ab initio* rotational constants agree very well with the experimentally determined values, exhibiting $\Delta(B_{\text{eff}})$ of 12–14 MHz (approximately 0.1%) for the HONC isotopologues.

In Table II, we summarize the harmonic ω_i frequencies, the fundamental ν_i frequencies computed from the anharmonic force field by second order perturbation theory, and the infrared intensities derived within the double harmonic approximation. Table III provides the centrifugal distortion constants in Watson's S reduction. These two tables furnish additional information, potentially useful for future high-resolution rotational spectroscopic studies on vibrationally excited HONC.

In accord with Table II, the most intense infrared transitions are to be expected in the region of the stretching ν_1(H–O) frequency, followed by the ν_3(H–O–N bend) transition of an almost halved intensity. The (ν_5, ν_6) wave number pair for the heavy-atom bending ν_5 mode and the torsional ν_6 mode calculated to be $(321\ cm^{-1}, 273\ cm^{-1})$ for HONC is smaller than both $(576\ cm^{-1}, 650\ cm^{-1})$ for HNCO and $(448\ cm^{-1}, 504\ cm^{-1})$ for HOCN.[40] Although the ν_5 and ν_6 modes of HONC possess a very low infrared spectral intensity in Table II, they are important in both the overall internal dynamics of real vibrating and rotating HONC (due to angular momentum conservation) and in the kinetic behavior (due to their major contribution to the number and density of states).

The vibrational ν_1 and ν_3 modes involve hydrogen and are sensitive to deuteration, see Table II. The intensity ratio $R_{\nu_1} = I_{\text{DO}}/I_{\text{HO}}$ of 0.50 for ν_1 readily indicates the highly localized nature of the OH(D) vibration. This can be demonstrated as follows. Making use of the normal coordinate Q_{XY} of the X-Y vibration written as $\sqrt{\mathcal{M}_{\text{XY}}}r(\text{X-Y})$ in the local mode picture, where $\mathcal{M}_{\text{XY}}$ is the reduced mass and r(X-Y) the internal coordinate, we may rewrite the intensity ratio

TABLE III. Centrifugal distortion constants (in megahertz) of Watson's S-reduced Hamiltonian, obtained from the CCSD(T)/cc-pCVTZ calculations by the use of perturbation theory.

Property	HONC	DONC	$HON^{13}C$	$HO^{15}NC$	$H^{18}ONC$
$10^3\ D_J$	5.79	4.90	5.30	5.79	5.34
D_K	325	43.2	332	355	356
D_{JK}	0.604	0.682	0.555	0.582	0.482
$10^4\ d_1$	−1.11	−1.39	−0.99	−1.13	−1.02
$10^4\ d_2$	−0.15	−0.39	−0.13	−0.15	−0.12

Downloaded 11 Nov 2012 to 129.132.209.87. Redistribution subject to AIP license or copyright; see http://jcp.aip.org/about/rights_and_permissions

$$R_{\nu_1} = |(d\mu/dQ_{\mathrm{DO}})_e|^2/|(d\mu/dQ_{\mathrm{HO}})_e|^2 \tag{4}$$

in the local mode limit as

$$^{lm}R_{\nu_1} = \mathcal{M}_{\mathrm{HO}}/\mathcal{M}_{\mathrm{DO}} = m_{\mathrm{H}}m_{\mathrm{DO}}/m_{\mathrm{D}}m_{\mathrm{HO}} = 0.53, \tag{5}$$

where m_{X} and m_{XY} denote the mass of X and XY, respectively. The theoretical R_{ν_1} value of 0.50 for HONC closely resembles the expected local mode result $^{lm}R_{\nu_1}$. Based on similar arguments and the bond-distance-bond-angle expression of the reduced mass for the bending vibration,[41] we obtain $R_{\nu_3}=0.63$ and $^{lm}R_{\nu_3}=0.57$ for ν_3, indicating a predominant local mode nature also for this bending mode. Inclusion of anharmonic contributions of the potential energy, in particular coupling with ν_2 and ν_1, may lead to a less localized character of ν_3; this can influence spectral intensities in the case of strong anharmonic resonances.

Pinnavaia *et al.*[4] suggested for the main isotopologue HONC a Fermi resonance of ν_2 with $2\nu_4$, a Coriolis resonance between ν_5 and ν_6, and a Darling–Dennison resonance of ν_5 with ν_6. In contrast, our *ab initio* calculations for the five HONC isotopologues leave room for a Fermi resonance of ν_2 with $2\nu_3$ only for DONC.

The centrifugal distortion constant D_J of 5.8 kHz for HONC in Table III is somewhat larger than $D_J=3.4$ kHz for HNCO and $D_J=4.1$ kHz for HOCN, obtained at the same CCSD(T)/cc-pCVTZ level of theory.[40] The constant D_K of 325 MHz for HONC is larger than $D_K=254$ MHz for HOCN,[40] but much smaller than the experimentally derived value $D_K=5940$ MHz for HNCO, known to be quasilinear.[42] The value of D_K is primarily defined by the quartic centrifugal distortion constant τ_{aaaa}, found to be -1303 and -176 MHz for, respectively, HONC and DONC, such that a decrease in D_K by a factor of 7.5 upon deuteration appears quite reasonable.

C. Nuclear quadrupole coupling constants

The nuclear quadrupole coupling constants χ_{ij} for the ^{14}N(I=1) and D(I=1) nuclei are computed at the CCSD(T)/cc-pCV5Z level of theory for the best CCSD(T) estimate structure of Fig. 2. These results are collected in Table IV. The theoretical results for χ_{ij} are not vibrationally averaged. Nuclear quadrupole coupling constants computed for HONC at the optimum CCSD(T)/cc-pCV5Z geometry were already reported in Table 2 of Ref. 7. The latter structure and the best CCSD(T) estimate structure of Fig. 2 agree within 0.0003 Å and 0.06°,[30] yielding nuclear quadrupole constants that agree within 1 kHz.

At the site of a specific nucleus A, the electric field gradient tensor q in the principal a,b,c axis system was computed first. The multiplication of the q_{ij} components by the nuclear quadrupole moment $Q(A)$ of the nucleus A provides the quadrupole coupling tensor χ,

$$\chi_{ij}(\mathrm{A}) = [eQ(\mathrm{A})/h]q_{ij}(\mathrm{A}), \tag{6}$$

at the site of A for $i,j=a,b,c$, where e and h denote the elementary charge and Planck's constant, respectively. The tensors χ and q are symmetric and traceless, such that e.g., $\chi_{ii}+\chi_{jj}+\chi_{kk}=0$ holds. From Eq. (6), we obtain

TABLE IV. Nuclear quadrupole coupling constants $\chi_{\alpha\beta}(^{14}\mathrm{N})$ and $\chi_{\alpha\beta}(\mathrm{D})$ (in megahertz) obtained experimentally (superscript exp) and computed from the correlated CCSD(T)/cc-pCV5Z density matrices at the best estimate structure displayed in Fig. 2. The numbers in parentheses given along with the experimental values are the estimated uncertainties (1σ) in units of the last significant digit. For the definition of $\Delta\chi_{aa}$ and the angles δ_{iso} and θ, see the main text (Sec. II C).

Property	HONC	DONC	HON^{13}C	H^{18}ONC
$^{\mathrm{exp}}\boldsymbol{\chi_{aa}}(^{14}\mathbf{N})$	**3.267(4)**	**3.238(5)**	**3.268(4)**	**3.271(4)**
$\chi_{aa}(^{14}\mathrm{N})$	3.224	3.196	3.224	3.227
$\Delta\chi_{aa}$		0.028	0.0	−0.003
$\chi_{bb}(^{14}\mathrm{N})$	−1.854	−1.826	−1.853	−1.857
$\chi_{ab}(^{14}\mathrm{N})$	−0.474	−0.604	−0.476	−0.457
$\chi_{cc}(^{14}\mathrm{N})$	−1.370	−1.370	−1.370	−1.370
δ_{iso}		1.5	0.0	0.2
$\theta(\alpha,a)$	174.7	173.2	174.7	174.9
$\theta(\alpha,\mathbf{r}_{\mathrm{ON}})$	0.4	0.4	0.4	0.4
$^{\mathrm{exp}}\boldsymbol{\chi_{aa}}(\mathbf{D})$		**−0.063(8)**		
$\chi_{aa}(\mathrm{D})$		−0.056		
$\chi_{bb}(\mathrm{D})$		0.229		
$\chi_{ab}(\mathrm{D})$		0.142		
$\chi_{cc}(\mathrm{D})$		−0.172		
$\theta(\alpha,a)$		67.6		
$\theta(\alpha,\mathbf{r}_{\mathrm{DO}})$		177.4		

$$\chi_{ij}(^{14}\mathrm{N})\ [\mathrm{MHz}] = 4.802\,68\ q_{ij}(^{14}\mathrm{N})[E_h/a_0^2] \tag{7}$$

and

$$\chi_{ij}(\mathrm{D})\ [\mathrm{MHz}] = 0.672\,00\ q_{ij}(\mathrm{D})[E_h/a_0^2] \tag{8}$$

using $Q(^{14}N)=2.044$ fm^2 and $Q(D)=0.286$ fm^2, both taken from a "year-2008" compilation of the known spectroscopic nuclear quadrupole moments by Pyykkö.[43]

The diagonalization of the nuclear quadrupole coupling tensor yields the eigenvalues $\chi_{\alpha\alpha},\chi_{\beta\beta},\chi_{\gamma\gamma}$, defined such that $|\chi_{\alpha\alpha}|\geq|\chi_{\beta\beta}|\geq|\chi_{\gamma\gamma}|$, which provide the asymmetry parameter η introduced as

$$\eta = (\chi_{\gamma\gamma}-\chi_{\beta\beta})/\chi_{\alpha\alpha}. \tag{9}$$

The latter parameter quantifies the deviation from a cylindrical charge distribution about a specific nucleus. At the site of nitrogen, the eigenvalues of the tensor χ are calculated to be $\chi_{\alpha\alpha}(^{14}\mathrm{N})=3.268$ MHz, $\chi_{\beta\beta}(^{14}\mathrm{N})=-1.898$ MHz, and $\chi_{\gamma\gamma}(^{14}\mathrm{N})=-1.370$ MHz, giving thus $\eta(^{14}\mathrm{N})$ of 0.16. For deuterium, we obtain eigenvalues of $\chi_{\alpha\alpha}(\mathrm{D})=0.287$ MHz, $\chi_{\beta\beta}(\mathrm{D})=-0.172$ MHz, and $\chi_{\gamma\gamma}(\mathrm{D})=-0.115$ MHz, such that $\eta(\mathrm{D})=0.20$. Nonzero values of η are characteristic of nonlinear bonds.

In Table IV, we also provide the angle $\theta(\alpha,a)$ between the inertial a axis and the principal quadrupole α axis, as well as the angle δ_{iso} between the a axis of HONC and the a axis of its isotopologues. The angles $\theta(\alpha,\mathbf{r}_{\mathrm{ON}})$ and $\theta(\alpha,\mathbf{r}_{\mathrm{HO}})$ of the principal quadrupole α axis with the bond distance vectors $\mathbf{r}_{\mathrm{ON}}=\mathbf{r}_{\mathrm{O}}-\mathbf{r}_{\mathrm{N}}$ and $\mathbf{r}_{\mathrm{DO}}=\mathbf{r}_{\mathrm{D}}-\mathbf{r}_{\mathrm{O}}$ are listed for the ^{14}N and D case, respectively. As seen in the table, the principal α axis almost coincides with $\mathbf{r}_{\mathrm{ON}}$ in the case of ^{14}N and with $\mathbf{r}_{\mathrm{DO}}$ in the case of deuterium.

In Table IV, the theoretical values for χ_{aa} agree with the experimental results $^{\mathrm{exp}}\chi_{aa}$ within 42–44 kHz for the ^{14}N

Downloaded 11 Nov 2012 to 129.132.209.87. Redistribution subject to AIP license or copyright; see http://jcp.aip.org/about/rights_and_permissions

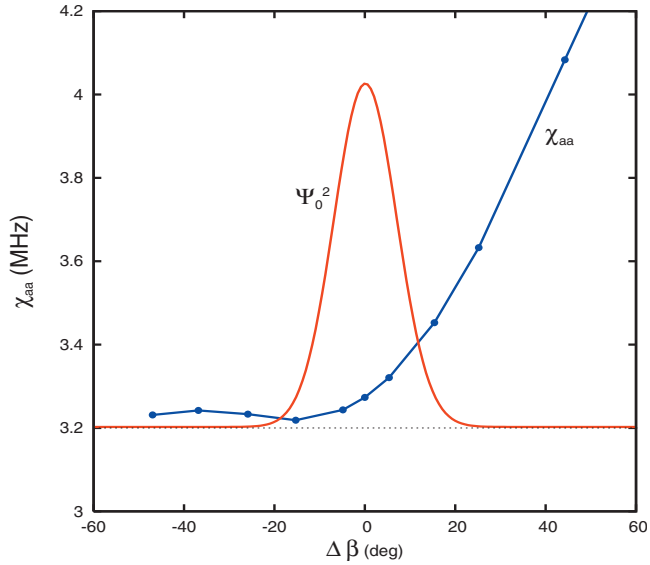

FIG. 3. Variation of the nitrogen nuclear quadrupole coupling constant $\chi_{aa}(^{14}\mathrm{N})$ of HONC along the minimum energy path in the direction of the bending angle β involving hydrogen. Here, $\Delta\beta$ stands for the displacement $\beta-\beta_e$ from the equilibrium value β_e. The ground-state wave function probability amplitude Ψ_0^2 obtained from the corresponding one-dimensional calculation is additionally displayed.

nucleus and within 7 kHz for deuterium. One may additionally note that the experimental and theoretical findings show the same trend with respect to the main species, $\mathrm{H}\,^{16}\mathrm{O}^{14}\mathrm{N}^{12}\mathrm{C}$, as seen with the help of

$$\Delta\chi_{aa} = \chi_{aa}(\mathrm{HONC}) - \chi_{aa}(\mathrm{isotope}). \tag{10}$$

The theoretical $\Delta\chi_{aa}$ values of 28, 0, and −3 kHz for nitrogen are in excellent agreement with the experimental $\Delta\chi_{aa}$ results of 29, −1, and −4 kHz obtained for, respectively, DONC, $\mathrm{HON}^{13}\mathrm{C}$, and $\mathrm{H}^{18}\mathrm{ONC}$.

The magnitude of the nitrogen nuclear quadrupole coupling constant $|\chi_{aa}(^{14}\mathrm{N})|$ for HONC is larger than the respective values of 2.114, 2.872, and 0.245 MHz found for HNCO, HOCN, and HCNO, respectively.[7] The principal quadrupole component $\chi_{cc}(^{14}\mathrm{N})$ is negative for HONC; to be compared with −1.559, 0.795, and −0.147 MHz for HNCO, HOCN, and HCNO, respectively.[7]

The nuclear quadrupole constants of HONC are now compared with the corresponding values for HNC. A recent theoretical CCSD(T)/cc-pCVTZ result for the equilibrium $\chi_{aa}(^{14}\mathrm{N})$ of HNC is given as 0.353 MHz.[44] Our CCSD(T)/aug-cc-pCVQZ value for this molecule amounts, however, to $\chi_{aa}(^{14}\mathrm{N})=0.317$ MHz, whereas we obtain $\chi_{aa}(\mathrm{D})$ of 0.279 MHz. In any case, we see that the equilibrium nuclear quadrupole constants for HONC appear to be one order of magnitude larger than those of HNC, exhibiting also a different sign in the case of $\chi_{aa}(\mathrm{D})$. For the ground vibrational state of HNC, Wong[44] computed $\chi_{aa}(^{14}\mathrm{N})$ of 0.296 MHz, which is thus by approximately 60 kHz (16%) smaller than his equilibrium result due to vibrational averaging. The experimentally derived $\chi_{aa}(^{14}\mathrm{N})$ and $\chi_{aa}(\mathrm{D})$ values for the ground vibrational state of HNC are reported to be 0.264 MHz and 0.262 MHz, respectively.[45]

In the case of nonlinear HONC, vibrational averaging may be expected to play a somewhat less important role since HONC possesses a pronounced barrier to linearity of ca. 16 700 cm^{-1}, as seen in Fig. 3 of Ref. 30, which shows the CCSD(T)/cc-pVQZ minimum energy path (MEP) along the bond angle HON of HONC. The variation of $\chi_{aa}(^{14}\mathrm{N})$ along this MEP depicted in Fig. 3 shows a steep increase of more than 1 MHz in $\chi_{aa}(^{14}\mathrm{N})$ upon straightening of the bending angle involving hydrogen. One-dimensional calculations carried out for β in the framework of the orthogonal diatom-diatom description of the internal molecular geometry[46] give an estimate of +15 kHz (0.5%) for the ground-state vibrational correction to $\chi_{aa}(^{14}\mathrm{N})$ due to this bending mode. The heavy-atom bending vibration does not contribute much to the vibrational averaging, since $\chi_{aa}(^{14}\mathrm{N})$ exhibits only a negligible variation of several kilohertz along the corresponding minimum energy path. More details on these calculations will be published elsewhere.[40]

D. Electron density

The nuclear quadrupole coupling constant is the spectroscopic measure of the interaction between the nuclear quadrupole moment and the molecular electric field gradient at the specific nuclear site. To qualitatively understand this effect, as well as a possible binding mechanism, several results regarding the electron subspace of HONC are presented here. For more details on this topic, see Ref. 7.

The individual basis function (orbital) populations are given in Table V, where p_z and p_y are the in-plane p orbitals, whereas p_x stands for the out-of-plane functions. The table clearly shows a decrease in the p_z and s characters and an increase in the p_x and p_y characters for both nitrogen and oxygen with respect to the free atom situation. This is an indication of a hybridization involving p orbitals[47] (π type binding). Although the orbital population at the carbon center is almost unchanged with respect to free C, a small increase of 0.08 electrons for p_z of C indicates some sp hybridization.

The nuclear quadrupole interaction results from the nonspherical charge distribution over hybrid orbitals,[47,48] the spherically symmetric closed-shell s electrons contributing nothing.[48] In accord with Fig. 4 showing the total electron distribution and Table V, a nearly cylindrically symmetric electron distribution in the valence shell of nitrogen and

TABLE V. Population analysis of the total CCSD(T)/cc-pCV5Z electron density by the basis function type.

Center	s	p_z	p_y	p_x	Total	Charge
H	0.59	0.02	0.02	0.05	0.69	+0.31
O	3.79	1.08	1.45	1.83	8.24	−0.24
N	3.25	0.82	1.35	1.31	6.86	+0.14
C	4.04	0.74	0.61	0.68	6.21	−0.21

Downloaded 11 Nov 2012 to 129.132.209.87. Redistribution subject to AIP license or copyright; see http://jcp.aip.org/about/rights_and_permissions

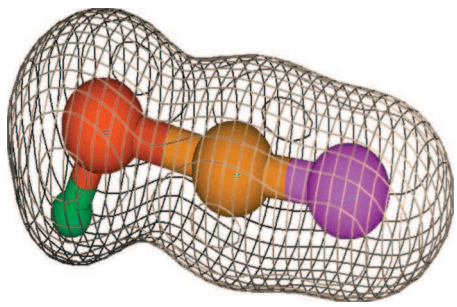

FIG. 4. Total electron density of HONC. The contour surface of magnitude 0.025 a.u. is shown.

largely asymmetric electron distribution in the valence shell of oxygen may readily be expected for HONC, resulting in an electric field gradient component $q_{aa}(^{14}\mathrm{N})$ of 0.671 E_h/a_0^2 markedly smaller than $q_{aa}(^{17}\mathrm{O})$ of 2.417 E_h/a_0^2. Since the magnitude of the nuclear quadrupole moment $Q(^{17}\mathrm{O})$ of -2.558 fm^2 (Ref. 43) is comparable to $Q(^{14}\mathrm{N})$, it follows $|\chi_{aa}(^{14}\mathrm{N})| < |\chi_{aa}(^{17}\mathrm{O})|$, as verified by our calculations reported elsewhere,[7] where we find $\chi_{aa}(^{17}\mathrm{O})$ of -14.51 MHz.

The highest occupied bonding molecular $9a'$ orbital of HONC is compared with the highest occupied molecular $5\sigma^+$ orbital of HNC in Fig. 5. The molecular $9a'$ orbital of HONC at -0.491 E_h lies 0.023 E_h below the highest occupied nonbonding out-of-plane $2a''$ orbital at -0.468 E_h shown in Fig. 1. The molecular orbitals of Fig. 5 are very similar, both clearly exhibiting a promotion of p_z electrons from nitrogen toward carbon and an electron cloud on carbon. In consequence, HONC and HNC possess similar equilibrium r_e(CN) bond lengths [1.173 Å versus 1.169 Å (Ref. 34)] due to a similar type of binding, schematically described as $\mathrm{N}^+ \equiv \mathrm{C}^-$.

Figure 5, as well as Figs. 1 and 4, were drawn with the help of the pre- and postprocessing program MOLDEN.[49]

III. LABORATORY MEASUREMENTS AND RESULTS

The rotational spectrum of HONC was detected with the same Fourier transform microwave spectrometer[50] used to detect cyanic acid, HOCN, and many other reactive molecules of chemical and astronomical interest. Many of these

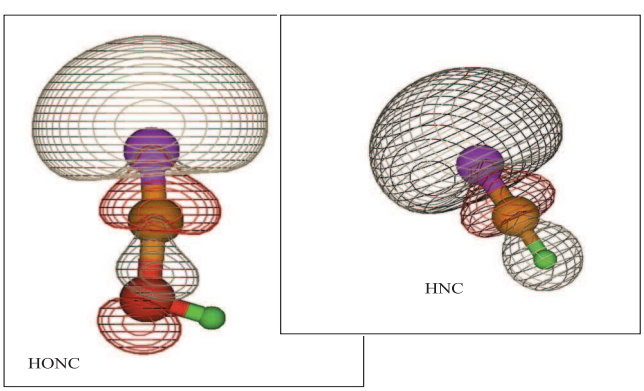

FIG. 5. Highest occupied bonding molecular $9a'$ orbital of HONC (left) and highest occupied molecular $5\sigma^+$ orbital of HNC (right). The contour surfaces of magnitude 0.025 and -0.025 are shown.

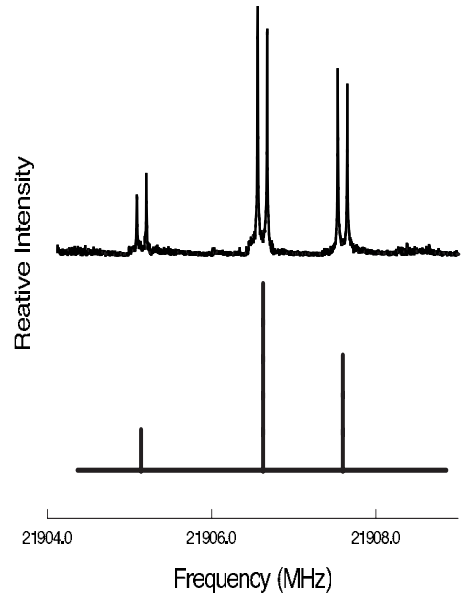

FIG. 6. Observed (top) and calculated (bottom) spectrum of the fundamental rotational transition of HONC, showing well resolved nitrogen hyperfine structure. The observed spectrum is a synthesis of several settings of the Fabry–Pérot cavity which, owing to the high-Q of the cavity at this frequency ($Q \sim 10\,000$), differ in frequency by 0.3 MHz. Each hyperfine component has a double-peaked line shape, the result of the Doppler shift of the Mach 2 molecular beam relative to the two traveling waves that compose the confocal mode of the Fabry–Pérot. The total integration time was 5 min. Shown beneath the observed spectrum is a calculated stick diagram derived from the best-fit constants in Tables I and IV.

are radicals and carbenes, but positively and negatively charged species have been studied as well. Reactive molecules are created in the throat of a small supersonic nozzle by applying a low-current dc discharge to a short gas pulse created by a fast mechanical valve.

Like fulminic and cyanic acid, isofulminic acid is a closed-shell asymmetric rotor near the prolate limit ($\kappa = -0.9994$), with a nearly linear heavy-atom backbone closely parallel to the a inertial axis (see Fig. 2), and a large rotational constant A (see Table I). Both intrastack a-type ($\Delta K_a = 0$) and interstack b-type ($\Delta K_a = \Delta K_c = \pm 1$) rotational transitions are allowed, and the calculated dipole moments along the two principal axes are fairly large ($\mu_a = 3.13$ D, $\mu_b = -1.54$ D; see Fig. 2). At the very low rotational temperature of our molecular beam ($T_{\mathrm{rot}} \sim 3$ K), however, only levels in the $K_a = 0$ ladder will be thermally populated, and the rotational spectrum of HONC simplifies to that of a linear molecule, with lines separated in frequency by approximately $(B+C) \sim 22$ GHz. Because of the relatively low frequency ceiling of our FTM spectrometer (<42 GHz), only the fundamental rotational transition ($1_{0,1} \rightarrow 0_{0,0}$) of HONC and its isomers is accessible with our present instrumentation. At the high spectral resolution (of order 0.1 ppm) which is readily achieved in our molecular beam experiments, however, the fundamental rotational line of HONC should possess a readily identifiable spectral fingerprint: a closely spaced, but well-resolved triplet with a characteristic 1:5:3 intensity ratio between the three lines, owing to nitrogen quadrupole hyperfine structure.

Our laboratory search for HONC was guided by rota-

Downloaded 11 Nov 2012 to 129.132.209.87. Redistribution subject to AIP license or copyright; see http://jcp.aip.org/about/rights_and_permissions

TABLE VI. Measured hyperfine structure in the fundamental rotational transition of HONC, $H^{18}ONC$, and $HON^{13}C$ (in megahertz).

$F' \rightarrow F$[a]	HONC	$HON^{13}C$	$H^{18}ONC$
$1 \rightarrow 1$	21 905.146	21 054.962	20 814.337
$2 \rightarrow 1$	21 906.620	21 056.435	20 815.813
$0 \rightarrow 1$	21 907.596	21 057.413	20 816.790

[a]Note—Estimated measurement uncertainties are 2 kHz.

tional constants derived from the high-level molecular structure calculations described in Sec. II B. Because zero-point corrections are generally small, the equilibrium (B_e) and vibrationally corrected (B_0) rotational constants differ by less than 0.4%, which amounts to a search of at most ±80 MHz near 21.9 GHz. Before undertaking the search, the discharge conditions were optimized on the corresponding transition of HNCO, which was produced in a 800 V dc discharge in the throat of the supersonic nozzle of the spectrometer through a mixture of water (0.035%), and cyanogen (NCCN, 0.03%) heavily diluted in neon. Typical gas flow rates were 30 cm^3/min at standard temperature and pressure at a 6 Hz pulse repetition rate, with pulses 300 μs in duration, and a stagnation pressure of 2.5 ktorr behind the nozzle. Under these conditions, the fundamental rotational transition of HNCO (22.0 GHz) is very intense, but the same line of HOCN (21.0 GHz) and HCNO (22.9 GHz) is also readily observed.

Only one unidentified triplet (see Fig. 6 and Table VI) was found in the search, and it almost certainly arises from HONC because (1) the measured frequency is very close to that calculated from two high-level *ab initio* equilibrium structure calculations, lying 0.12% lower than that predicted in Table I, and 0.10% lower than that predicted by Schuurman *et al.*[5] at a similarly high level of theory and (2) the measured quadrupole coupling constant χ_{aa}=3.267 MHz is extremely close to that predicted (3.224 MHz; Table IV). Additional evidence of the identification is provided by the observation of the same transition of $H^{18}ONC$, $HO^{13}NC$, and DONC at the expected isotopic shifts with essentially the same χ_{aa} as that measured for the normal species. For DONC, additional quadrupole hyperfine structure from the deuterium was resolved (Table VII), and as Table IV shows the theoretical and experimental quadrupole coupling constants for deuterium and nitrogen are in excellent agreement. For the $H^{18}ONC$ isotopic measurements, $^{18}O_2$ was used as a precursor gas together with methyl cyanide (CH_3CN); for $HON^{13}C$, carbon-13 methyl cyanide ($CH_3{}^{13}CN$) was used with water; and for DONC, heavy water (D_2O) was used with cyanogen. A search for $HO^{15}NC$ was also undertaken using methanol and $^{15}N_2$, and several lines were found near the predicted isotopic shift; owing to the lack of quadrupole moment for ^{15}N, it was not possible to unambiguously identify which line arises from this isotopic species.

TABLE VII. Measured hyperfine structure in the fundamental rotational transition of DONC (in megahertz).

$F_1' \rightarrow F_1$	$F' \rightarrow F$	Frequency[a]
$1 \rightarrow 1$	$1 \rightarrow 0$	20 822.026
	$1 \rightarrow 1$	20 822.026
	$1 \rightarrow 2$	20 822.026
$2 \rightarrow 1$	$2 \rightarrow 1$	20 823.477
	$2 \rightarrow 2$	20 823.477
	$3 \rightarrow 2$	20 823.490
	$1 \rightarrow 0$	20 823.498
	$1 \rightarrow 1$	20 823.498
	$1 \rightarrow 2$	20 823.498
$0 \rightarrow 1$	$0 \rightarrow 1$	20 824.441
	$2 \rightarrow 1$	20 824.454
	$2 \rightarrow 2$	20 824.454
	$1 \rightarrow 0$	20 824.464
	$1 \rightarrow 1$	20 824.464
	$1 \rightarrow 2$	20 824.464

[a]Note—Estimated measurement uncertainties are 3 kHz.

IV. DISCUSSION

The present work firmly establishes the existence of the elusive isofulminic acid, and will permit a comparative study of all four isocyanic isomers. Although the data set is limited for HONC, with the isotopic data in hand, an experimental r_0 structure for this bent chain can be derived assuming a nearly linear heavy-atom ONC backbone $\angle(\mathrm{ONC})=172.6°$ and $\angle(\mathrm{HON})=105°$. On this basis we derive bond lengths of $r^0_{\mathrm{CN}}=1.177(3)$ Å, $r^0_{\mathrm{NO}}=1.333(3)$ Å, and $r^0_{\mathrm{OH}}=0.958(3)$ Å. Making use of the ground-state vibrational corrections $\Delta B^{(3)}$ and $\Delta C^{(3)}$ from Table I in combination with the experimental results B_{eff}, we obtain experimental equilibrium r_e bond lengths given by $r^e_{\mathrm{CN}}=1.1744(4)$ Å, $r^e_{\mathrm{NO}}=1.3304(4)$ Å, and $r^e_{\mathrm{OH}}=0.9605(4)$ Å. The latter results are in good agreement (to better than ±0.005 Å) with those predicted from theory, Fig. 2, providing thus a further evidence that the real "carboxime"[51] with the structure HO–N≡C has indeed been found. Analytical expressions for the principal moments of inertia in the bond-distance-bond-angle description and for their partial derivatives with respect to the geometrical parameters were employed here in combination with a Levenberg–Marquardt nonlinear least-squares algorithm[52] to compute the experimental equilibrium bond lengths r^e_{CN}, r^e_{NO}, and r^e_{OH}.

It is rather remarkable that isofulminic acid, calculated to lie 84 kcal/mol or nearly 4 eV above isocyanic acid, is readily produced in electric discharges starting from a wide variety of precursor gases containing H, C, N, and O. We estimate from line intensities that abundances relative to HNCO are 12% for HOCN, 2% for HCNO, and 1% for HONC in the molecular beam. Now that all four isocyanic isomers have been detected spectroscopically, it may be worthwhile to systematically measure relative abundances with different precursor combinations. Such a study might clarify the production routes that are operative in our discharge source.

Now that a simple but fairly efficient method for *in situ* synthesis of HONC has been demonstrated here, it should be possible to extend present work to the millimeter and submillimeter wavelengths to determine individual rotational and centrifugal distortion constants. Because HONC possesses a sizable dipole moment along the *b*-axis

Downloaded 11 Nov 2012 to 129.132.209.87. Redistribution subject to AIP license or copyright; see http://jcp.aip.org/about/rights_and_permissions

(μ_b=−1.54 D), a precise determination of the A rotational constant should be possible. The IR vibrational spectrum of HONC is also of interest to test theoretical models of the potential energy surface and to determine the extent of quasilinearity for this highly energetic isomer. The calculated fundamental vibrational frequencies, infrared intensities, and centrifugal distortion constants in Tables II and III should serve as a useful guide.

Ground state rotational constants derived from coupled cluster calculations here and elsewhere agree to ~0.1% or better with those measured for HONC and its three isomers, and a nearly comparable level of accuracy was recently achieved for another set of closed-shell molecules, the carbon-chain anions $C_{2n}H^-$ (n=1–4),[53–55] CN^-,[56] and C_3N^-.[57] Such close agreement suggests that the same theoretical methods might be applied to predict accurate spectroscopic constants for many other closed-shell molecules. It remains to be seen if 0.1% is the limit of present theory or not, and to critically assess if theoretical methods can be refined even further, perhaps by a factor of 10 or more, i.e., 0.01%. Even at the present level of accuracy, theoretical spectroscopic constants are an extremely helpful aid in the assignment of rotational spectra: they significantly reduce the frequency range of a laboratory search and well predict hyperfine structure.

Because HOCN and HCNO have recently been identified in space, detection of HONC is not out of the realm of possibility. It is calculated to lie only 14 kcal/mol higher in energy than HCNO and is comparably polar, so it may be found in warm regions where HCNO is abundant. If detected in space, the abundance ratios between HONC and other isomers may provide further insight into the complex gas and surface chemistry, which is thought to produce these isomers. The discovery of HCNO in space, for example, led Marcelino *et al.*[17] to suggest that $CH_2+NO \rightarrow HCNO+H$ is a key reaction in the formation of fulminic acid, allowing them to reproduce the observed abundances of HCNO in both dark clouds and the low-mass star forming core L1527.

ACKNOWLEDGMENTS

M.M. and M.L. kindly acknowledge the access to the high performance computers of the Institut du Développement et des Ressources en Informatique Scientifique (IDRIS) through Grant No. 82170. The work in Cambridge is supported by NSF grant (Grant No. CHE-0701204) and NASA grant (Grant No. NNX08AE05G).

[1] J. H. Teles, G. Maier, B. A. Hess, Jr., L. J. Schaad, M. Winnewisser, and B. P. Winnewisser, Chem. Ber. **122**, 753 (1989) (and references therein).
[2] A. D. McLean, G. H. Loew, and D. S. Berkowitz, J. Mol. Spectrosc. **64**, 184 (1977).
[3] D. Poppinger, L. Radom, and J. A. Pople, J. Am. Chem. Soc. **99**, 7806 (1977).
[4] N. Pinnavaia, M. J. Bramley, M.-D. Su, W. H. Green, and N. C. Handy, Mol. Phys. **78**, 319 (1993).
[5] M. S. Schuurman, S. R. Muir, W. D. Allen, and H. F. Schaefer III, J. Chem. Phys. **120**, 11586 (2004).
[6] M. Mladenović and M. Lewerenz, Chem. Phys. **343**, 129 (2008).
[7] M. Mladenović, M. Elhiyani, and M. Lewerenz, J. Chem. Phys. **131**, 034302 (2009).
[8] D. Buhl, L. E. Snyder, and J. Edrich, Nature (London) **243**, 513 (1973).
[9] R. Kewley, K. V. L. N. Sastry, and M. Winnewisser, J. Mol. Spectrosc. **10**, 418 (1963).
[10] J. M. Jackson, J. T. Armstrong, and A. H. Barrett, Astrophys. J. **280**, 608 (1984).
[11] N. Q. Rieu, C. Henkel, J. M. Jackson, and R. Mauersberger, Astron. Astrophys. **241**, L33 (1991).
[12] I. Zinchenko, C. Henkel, and R. Q. Mao, Astron. Astrophys. **361**, 1079 (2000).
[13] M. Wang, C. Henkel, Y.-N. Chin, J. B. Whiteoak, M. H. Cunningham, R. Mauersberger, and D. Muders, Astron. Astrophys. **422**, 883 (2004).
[14] S. Martín, M. A. Requena-Torres, J. Martín-Pintado, and R. Mauersberger, Astrophys. J. **678**, 245 (2008).
[15] S. Brünken, C. A. Gottlieb, M. C. McCarthy, and P. Thaddeus, Astrophys. J. **697**, 880 (2009).
[16] S. Brünken, A. Belloche, S. Martín, L. Verheyen, and K. M. Menten, "Interstellar HOCN in the Galactic center region," Astron. Astrophys. (submitted).
[17] N. Marcelino, N. J. Cernicharo, N. B. Tercero, and E. Roueff, Astrophys. J. **690**, L27 (2009).
[18] B. P. Winnewisser, in *Molecular Spectroscopy: Modern Research*, edited by K. N. Rao (Academic, Orlando, 1985), Vol. 3, p. 321 (and references therein).
[19] M. Winnewisser, B. P. Winnewisser, I. R. Medvedev, F. C. De Lucia, S. C. Ross, and L. M. Bates, J. Mol. Struct. **798**, 1 (2006) (and references therein).
[20] M. E. Jacox and D. E. Milligan, J. Chem. Phys. **40**, 2457 (1964).
[21] V. E. Bondybey, J. H. English, C. W. Mathews, and R. J. Contolini, J. Mol. Spectrosc. **92**, 431 (1982).
[22] G. Maier, J. H. Teles, B. A. Hess, Jr., and L. J. Schaad, Angew. Chem., Int. Ed. Engl. **27**, 938 (1988).
[23] G. Maier, A. Bothur, J. Eckwert, H. P. Reisenauer, and T. Stumpf, Liebigs. Ann. **1997**, 2505 (1997).
[24] C. Wentrup, B. Gerecht, and H. Briehl, Angew. Chem., Int. Ed. Engl. **18**, 467 (1979).
[25] D. McNaughton and C. J. Evans, Z. Phys. Chem. **214**, 1313 (2000).
[26] D. Poppinger and L. Radom, J. Am. Chem. Soc. **100**, 3674 (1978).
[27] C. Wentrup, B. Gerecht, D. Laqua, H. Briehl, H.-W. Winter, H. P. Reisenauer, and M. Winnewisser, J. Org. Chem. **46**, 1046 (1981).
[28] A. M. Mebel, A. Luna, M. C. Lin, and K. Morokuma, J. Chem. Phys. **105**, 6439 (1996).
[29] Y.-Q. Ding, D.-C. Fang, and R.-Z. Liu, Mol. Phys. **103**, 767 (2005).
[30] M. Mladenović, M. Elhiyani, and M. Lewerenz, J. Chem. Phys. **130**, 154109 (2009).
[31] J. F. Stanton, J. Gauss, J. D. Watts, P. G. Szalay, R. J. Bartlett with contributions from A. A. Auer, D. B. Bernholdt, O. Christiansen, M. E. Harding, M. Heckert, O. Heun, C. Huber, D. Jonsson, J. Jusélius, W. J. Lauderdale, T. Metzroth, C. Michauk, D. P. O'Neill, D. R. Price, K. Ruud, F. Schiffmann, M. E. Varner, J. Vázquez and the integral packages MOLECULE (J. Almlöf and P. R. Taylor), PROPS (P. R. Taylor), and ABACUS (T. Helgaker, H. J. Aa. Jensen, P. Jørgensen, and J. Olsen). For the current version, see http://www.aces2.de.
[32] T. H. Dunning, Jr., J. Chem. Phys. **90**, 1007 (1989).
[33] D. E. Woon and T. H. Dunning, Jr., J. Chem. Phys. **103**, 4572 (1995).
[34] R. A. Creswell and A. G. Robiette, Mol. Phys. **36**, 869 (1978).
[35] G. Herzberg, *Infrared and Raman Spectra of Polyatomic Molecules*, Molecular Spectra & Molecular Structure, Vol. II, (corrected reprint of 1945 edition) (Krieger, Malabar FL, 1991).
[36] W. H. Hocking, M. C. L. Gerry, and G. Winnewisser, Can. J. Phys. **53**, 1869 (1975).
[37] R. Takashi, K. Tanaka, and T. Tanaka, J. Mol. Spectrosc. **138**, 450 (1989).
[38] G. L. Blackman, R. D. Brown, P. D. Godfrey, and H. I. Gunn, Nature (London) **261**, 395 (1976).
[39] I. M. Mills, in *Molecular Spectroscopy: Modern Research*, edited by K. N. Rao and C. W. Mathews (Academic, New York, 1972), Vol. 3, p. 115.
[40] M. Mladenović, "Spectroscopic properties of the four most stable CHNO isomers from *ab initio* CCSD(T) studies," J. Chem. Phys. (in preparation).
[41] M. Mladenović, J. Chem. Phys. **112**, 1082 (2000).
[42] A. V. Lapinov, G. Y. Golubiatnikov, V. N. Markov, and A. Guarnieri, Astron. Lett. **33**, 121 (2007).
[43] P. Pyykkö, Mol. Phys. **106**, 1965 (2008).
[44] B. M. Wong, Phys. Chem. Chem. Phys. **10**, 5599 (2008).
[45] H. A. Bechtel, A. H. Steeves, and R. W. Field, Astrophys. J. **649**, L53

Downloaded 11 Nov 2012 to 129.132.209.87. Redistribution subject to AIP license or copyright; see http://jcp.aip.org/about/rights_and_permissions

(2006).
[46] M. Mladenović, J. Chem. Phys. **112**, 1070 (2000).
[47] B. P. Dailey, J. Phys. Chem. **57**, 490 (1953).
[48] C. H. Townes and B. P. Dailey, J. Chem. Phys. **17**, 782 (1949).
[49] G. Schaftenaar and J. H. Noordik, J. Comput.- Aided Mol. Des. **14**, 123 (2000).
[50] M. C. McCarthy, W. Chen, M. J. Travers, and P. Thaddeus, Astrophys. J., Suppl. Ser. **129**, 611 (2000) (and references therein).
[51] G. Maier, Pure Appl. Chem. **63**, 275 (1991).
[52] W. H. Press, B. P. Flannery, S. A. Teukolsky, and W. T. Vetterling, *Numerical Recipes* (Cambridge University Press, Cambridge, 1986).
[53] M. C. McCarthy, C. A. Gottlieb, H. Gupta, and P. Thaddeus, Astrophys. J. **652**, L141 (2006).
[54] H. Gupta, S. Brünken, F. Tamassia, C. A. Gottlieb, M. C. McCarthy, and P. Thaddeus, Astrophys. J. **655**, L57 (2007).
[55] S. Brünken, C. A. Gottlieb, H. Gupta, M. C. McCarthy, and P. Thaddeus, Astron. Astrophys. **464**, L33 (2007).
[56] C. A. Gottlieb, S. Brünken, M. C. McCarthy, and P. Thaddeus, J. Chem. Phys. **126**, 191101 (2007).
[57] M. C. McCarthy and P. Thaddeus, J. Chem. Phys. **129**, 054314 (2008).

Downloaded 11 Nov 2012 to 129.132.209.87. Redistribution subject to AIP license or copyright; see http://jcp.aip.org/about/rights_and_permissions